ELSEVIER

Journal of Non-Crystalline Solids 246 (1999) 115–127

JOURNAL OF NON-CRYSTALLINE SOLIDS

Surface and volume nucleation and growth in TiO_2–cordierite glasses

Vladimir M. Fokin, Edgar D. Zanotto *

Vitreous Materials Laboratory (LaMaV), Department of Materials Engineering (DEMa), Federal University of São Carlos (UFSCar), 13655-905 São Carlos-SP, Brazil

Received 23 September 1997; received in revised form 4 November 1998

Abstract

Systematic measurements and analyses of surface nucleation and growth of μ-cordierite on diamond-polished surfaces and on fractured surfaces of cordierite glasses containing 0.3, 1.2, 3.4, 6.2 and 8.1 wt% TiO_2 were carried out. All the glasses exhibit surface nucleation, however, the glass having 8.1 wt% TiO_2 also exhibits volume nucleation. The maximum surface nucleation rate is located at a temperature considerably higher than the maximum volume nucleation rate. Both surface and volume crystallization occur by heterogeneous nucleation. The average nucleus/substrate wetting angles, θ, were estimated from surface and volume nucleation measurements. The widely different values of θ indicate that the active catalyzing sites are different for surface and volume crystallization. It is likely that Al_2TiO_5 crystals induce volume crystallization of μ-cordierite, while surface crystallization is affected by TiO_2, defects and relicts of polishing power. Nucleation on fractured surfaces was induced mainly by solid particles, most likely by broken glass particles. The crystal growth velocity of μ-cordierite crystals is well fitted by the 2D-surface nucleation growth model.

1. Introduction

The kinetics of glass crystallization are usually described by means of crystal nucleation (I) and growth (U) rates. Both volume and surface crystallization can occur, depending on where nucleation initiates. In systems which display internal crystallization, nucleation on the external glass surfaces is more copious than volume nucleation due to a decreased thermodynamic barrier for nucleation on the surface.

A number of papers have been published recently on both experimental and theoretical investigations of surface nucleation, e.g. [1–4]. Several distinguishing features of surface crystallization have been found. Due to the significant activity of the Technical Committee Seven (TC-7) of the IGC, surface nucleation in cordierite glass has been investigated in detail [5–9]. It has been shown that surface nucleation occurs predominantly on some preferred active surface sites. Thus the number of pre-existing sites limits the nucleation process. To date, however, experimental values of both surface and volume nucleation rate in the *same glass* have been obtained only for soda-lime–silica glasses [10]. The surface was not described and nucleation kinetics were not analysed in Ref. [10].

The aim of the present paper is to study both surface and volume crystallization in a TiO_2–cordierite glass and analyze the nucleation and growth data within the framework of classical

* Corresponding author.

0022-3093/99/$ – see front matter
PII: S0022-3093(99)00007-1

nucleation theory and standard models of crystal growth.

2. Experimental

Samples of cordierite glasses with different TiO_2 contents were supplied by Drs R. Müller and M. Kirsh of the former ZINH (East Berlin), now BAM. The analyzed glass compositions are given in Table 1. Tables 2 and 3 list the values of microhardness and the VFT viscosity parameters. Double and single stage heat treatments were used to study volume nucleation, and single stage heat treatments to study surface nucleation and growth. The main equipment used were a transmitted polarised light microscope (Jenaval, Carl Zeiss/Jena), reflected light microscope (Neophot, Carl Zeiss/Jena) and (Nikon) with an image analyzer device (OPTOMAX-V). The systematic errors in the crystal number density, N_v, for the single treatments were smaller than 5%, while the statistical errors for both types of treatment were ~10–20%.

3. Nucleation kinetics

3.1. Surface nucleation

To evaluate the time dependence of number density $N_S(t)$ of crystals nucleated on the specimen surfaces, the $n_S(2R_k)$ crystal size distributions were constructed for each temperature. Here, $k = r, (r-1), \ldots, 3, 2, 1$ is the number of a class with an average crystal size $2R_k (R_r < R_{r-1} < R_2 < R_1)$. The average birth time t_k of class k crystals (average size $2R_k$) is given by Eq. (1):

$$t_k(T) = t_h - R_k/U(T), \tag{1}$$

where t_h is the heat treatment time at a temperature T and $U(T)$ is crystal growth rate at the same temperature. The number, N_S, of crystals nucleated on a glass surface for a given time $t_k \leqslant t_h$ can be calculated by the following equation:

$$N_S(t) = N_S(t_k) = \sum_{m=1}^{k} n_S(2R_m). \tag{2}$$

This approach to estimate surface nucleation kinetics was first applied in the study of metallic glasses [11].

Table 1
Analysed glass composition in wt%

Glass	SiO_2	Al_2O_3	MgO	TiO_2
N1	52.05	34.89	12.76	0.30
N2	50.92	34.49	13.38	1.21
N3	49.38	33.07	14.13	3.42
N4	48.75	32.51	12.56	6.18
N5	47.52	31.54	12.80	8.14

Table 2
Microhardness as a function of TiO_2 content

Glass	Vikers hardness
N1	655 ± 7
N2	657 ± 7
N3	657 ± 8
N4	661 ± 8
N5	655 ± 8

Table 3
Vogel–Fulcher–Tammann (VFT) parameters *

Glass	A	B	T_0	Temp. range
N1	−17.54	20 109	137.4	812–892
N2	−12.29	13 590	251.5	804–889
N3	−8.66	9205	350.9	790–860
N4	63.32	64 325	2036.2	778–838
N5	−4	5581	419.8	761–844

* $\log(\eta) = A + B/(T - T_0)$, η in Pa s, T in °C.
The viscosity was measured by the beam-bending method. The unusual values of T_0 for glass N4 only reflect the fact that the viscosity was determined in limited temperature ranges and thus this fitted curve cannot be used for extrapolations for wider temperature intervals.

3.1.1. Diamond paste-polished surfaces

We were able to distinguish two crystal morphologies on glass surfaces polished by a diamond paste: an extended form, which is close to an ellipse, and an isometric hexagonal form. According to the X-ray phase analysis both morphologies are related to μ-cordierite crystals. The growth velocity of the small axis of the isometric crystals is close to that of the ellipsoidal crystals. Therefore, the smallest crystal sizes, $2R_{min}$, of both morphologies mentioned above were used to build size distributions *common* to all morphologies.

Typical crystal size distributions for glasses with *low TiO_2 contents* ($\leqslant 1.2$ wt%), are shown in Fig. 1(a). Most of the distributions shift to larger sizes and slightly broader widths with heat treatment time. Thus, the size interval, from $2R = 0$ to $2R_r$ ($2R_r \gg \varepsilon$, the microscope resolution), increases. Extended treatments caused crystal growth but did not result in nucleation of new crystals. The kinetic curves $N_S(t)$, calculated from crystal size distributions, exhibit saturation (Fig. 1(b)). Therefore, all available active surface sites were exhausted after short heat treatments, ~30 min. It is clear that, generally, the saturation level, N_{st}, is close to the number of initial active sites on the surface. Hence, an apparent surface nucleation rate, I_S, can be estimated by the following equation [12]:

$$I_S = dN_S(t)/dt = [N_{st} - N_S(t)]I_t, \quad (3)$$

where $I(t)$ is the nucleation rate per active site, in other words, the probability of crystal nucleation on any active site per unit time.

For glasses having *high TiO_2 contents* ($\geqslant 3.4$ wt%), the minimum values, $2R_r$, of the crystal size is near the microscope resolution limit. Extending the heat treatment time results in increasing the area under the size distribution curve (Fig. 2a), which is equal to the total number of crystals. The corresponding kinetic curves, $N_S(t)$, demonstrate a continuously increasing number of crystals. Fig. 2(b) shows that no saturation was reached up to 40 min of treatment time. Similar results were obtained in [13] for a $Ni_{66}B_{34}$ glass. Further prolongation of heat treatment was restricted by impingement.

Fig. 3 shows the maximum values of the apparent surface nucleation rate $I_S = dN_S/dt|_{max}$, at

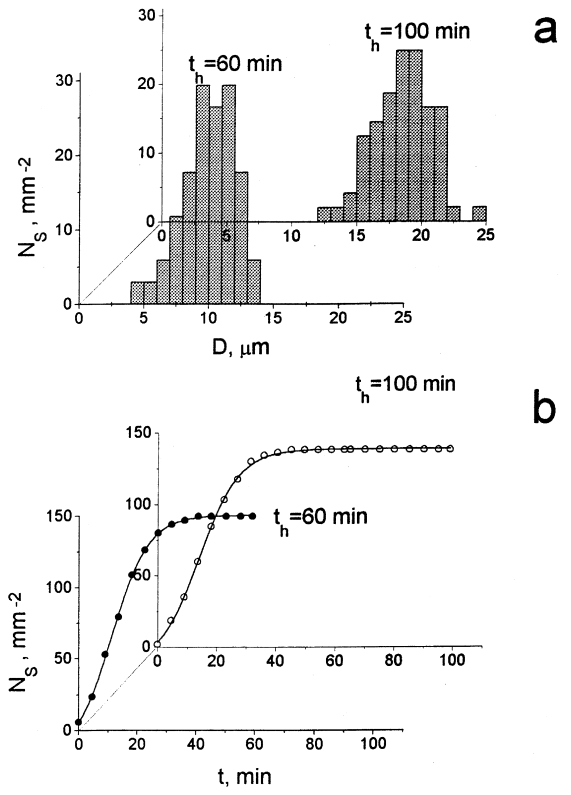

Fig. 1. Size distributions of μ-cordierite crystals on diamond polished surfaces of glass N2 after treatment at 890°C for 60 and 100 min (a); calculated kinetic curves (b).

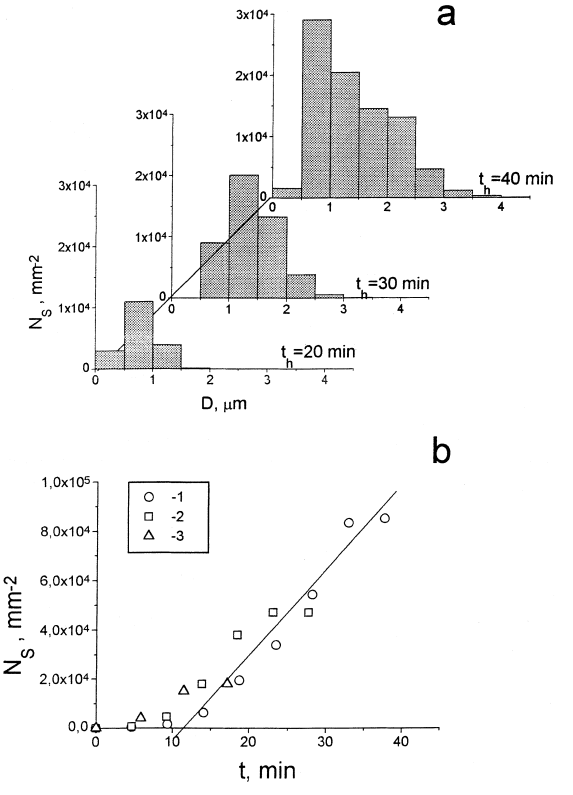

Fig. 2. Size distributions of μ-cordierite crystals on diamond-polished surfaces of glass N5 after treatment at 850°C for 20, 30 and 40 min (a); calculated kinetic curves (b): 1, 2,3 – $t_h = 40$, 30, and 20 min, respectively.

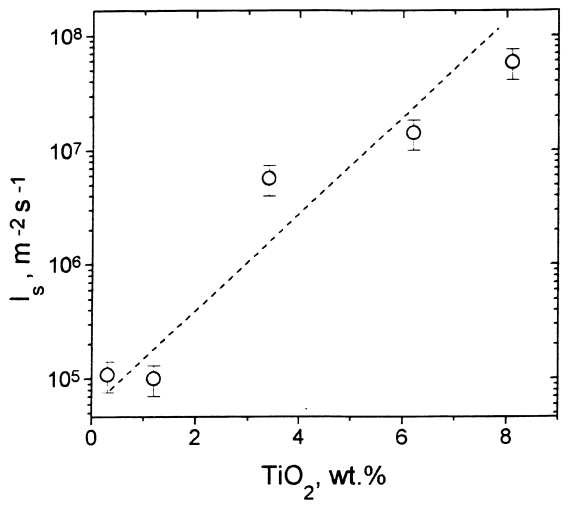

Fig. 3. Apparent surface nucleation rate at temperatures corresponding to a viscosity $\eta = 10^9$ Pa s as a function of TiO_2 content.

temperatures corresponding to a viscosity of $\eta = 10^9$ Pa s, as a function of TiO_2 content. A well-defined increase of I_S is observed. It should be stressed that volume nucleation is only observed in glasses having a high TiO_2 content, $TiO_2 \geqslant 8.1$ wt%. The other glass compositions only nucleated on the surfaces. It should also be emphasized that at this temperature range, 850°C, the volume nucleation rate in the 8.1 wt% TiO_2 glass is about 5 orders of magnitude smaller than the surface nucleation rate. Consequently, one would expect to observe about 0.5 crystals/mm^2 on the surface (traces from volume crystals) and 8×10^4 crystals/mm^2 resulting directly from surface nucleation. Thus, in this case, crystals that nucleate in the glass bulk did not interfere with surface nucleation measurements.

The differences indicated between the kinetic curves, $N_S(t)$, of glasses having low and high TiO_2 contents (Figs. 1 and 2) hinder the comparison of surface nucleation rates in glasses containing different amounts of TiO_2.

If the following condition is met:

$$N_S(t) \ll N_{st}, \tag{4}$$

Eq. (3) becomes

$$I_S = dN_S/dt \cong N_{st} I. \tag{5}$$

It may be suggested that Eq. (5) holds for high TiO_2 contents. If the nature and size of the active sites is not TiO_2 content dependent, the thermodynamic barrier for nucleation does not change with TiO_2 content. Hence, at temperatures of equal viscosity, the nucleation rate per active site, I, should be equal for the glasses with different TiO_2 content. In a situation such as this, it is natural to explain the enhancement of the apparent nucleation rate (I_S) mainly by an increase in the number of active sites. It should be noted that in the case of heterogeneous nucleation in a Pt-doped $Li_2O.2SiO_2$ glass, an increase of Pt content from 1 to 5 ppm resulted in an enhancement of nucleation rate but did not change the thermodynamic barrier [14].

Kinetic curves were also obtained at 830°C and 880°C for the glass having 8.1 wt% TiO_2 (N5). The corresponding values of $dN_S/dt|_{max}$ are presented in Fig. 4. Fig. 4 also shows values of $dN_S/dt|_{max}$ as a function of temperature obtained in [15] for μ-cordierite crystals on the surface of a TiO_2-free cordierite glass, polished by cerium oxide. The $I_S(T)$ plots for glass N5 and for the TiO_2-free cordierite glass demonstrate an increase of the apparent surface nucleation rate with temperature in the chosen temperature interval. An increase of surface nucleation rate, I, was also shown in [15] for μ-cordierite crystals.

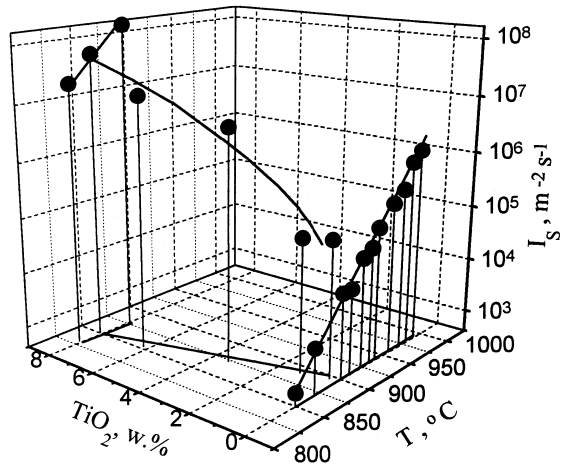

Fig. 4. Apparent surface nucleation rate as a function of TiO_2 content and temperature; data for TiO_2-free glass from Ref. [15].

3.1.2. Nucleation on fractured surfaces

The number density of μ-cordierite crystals on a fractured surface (0–20 mm^{-2}) is far less that on polished surfaces (10^2–10^5 mm^{-2}), and does not exhibit a clear dependence on the TiO_2 content. Practically all crystals have a solid particle of cordierite composition in the centre. Fig. 5 shows a typical crystal. It is likely that the central particle is a cordierite glass relict that constituted the original nucleation site.

3.2. Volume nucleation

Only the glass N5, having 8.1 wt% TiO_2, exhibits volume nucleation. It was shown in [16] that the maximum volume nucleation rate of μ-cordierite, I_v, of a glass of composition very close to the composition of glass N5 occurs at $T_{max} = 725°C < T_g \cong 772°C$. In the present work, volume nucleation rates $I_v = dN_v/dt$ of μ-cordierite were obtained at higher temperatures, beginning with $T = 750°C$, in order to compare them with the surface nucleation rates, $I_S = dN_S/dt$.

To obtain the kinetic dependencies of $N_v(t)$, double stage heat treatments were used for $T = 750°C$, 770°C and 800°C, while single stage treatments were used for higher temperatures ($T = 830°C$, 850°C and 870°C). After the heat treatments, polished plates approximately a 100–200 μm thick were analyzed to obtain the number of crystals per unit volume of glass, N_v, with transmission optical microscopes. Fig. 6 presents the temperature dependence of both (stationary) volume nucleation rate, I_v, and apparent surface nucleation rate, I_S. That figure clearly shows that the surface nucleation rate maximum occurs at temperatures considerably higher than that of maximum volume nucleation rate. (It is assumed that N_{st} does not depend strongly on the temperature of nucleation and hence, according to Eq. (5), $I(T) \sim I_S(T)$.)

4. Crystal growth velocity

In the case of nucleation and growth in the glass volume, the morphology of μ-cordierite crystals resembles a prolate ellipsoid. In *surface* nucleation and growth, the crystals resemble ellipses. Therefore, the crystal growth rates $U_{max} = dR_{max}/dt$ and $U_{min} = dR_{min}/dt$ were measured in the direction of the largest and the smallest axis, respectively. Fig. 7 shows plots of $\ln U_{max}$ and $\ln U_{min}$ for glass N5 versus inverse temperature. It also presents the growth rate of hexagonal isometric prisms of α-cordierite nucleated in the interior of the glass. It should be noted that the growth rate of μ-cordierite in the glass bulk is very close to that on the polished glass surface (see $T = 880°C$, 850°C, and 830°C in Fig. 7).

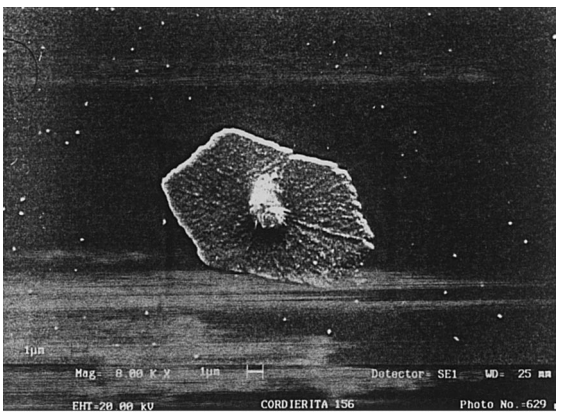

Fig. 5. SEM micrograph of a μ-cordierite crystal on a fractured surface of glass N4 treated for 180 min at 853°C.

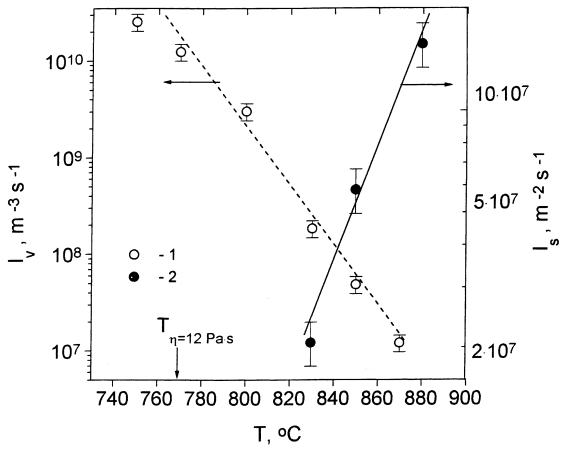

Fig. 6. Stationary volume nucleation rate I_v (1) and apparent surface nucleation rate I_S (2) in glass N5 as function of temperature. Straight lines are placed just to guide the eye.

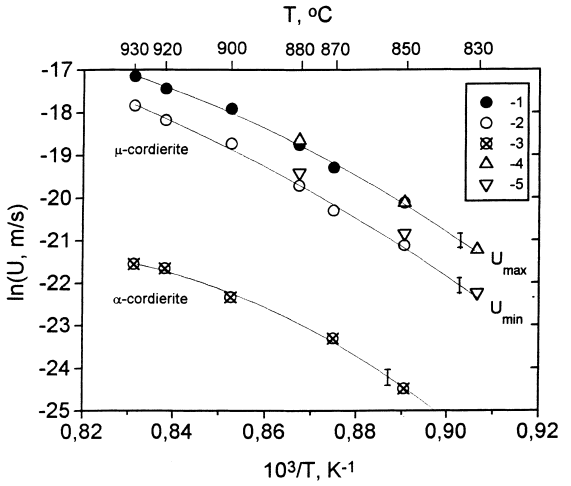

Fig. 7. Growth velocity of μ-cordierite (1, 2, 4, 5) and α-cordierite (3) in glass N5: 1 – U_{max}(vol.); 2 – U_{min}(vol.); 4 – U_{max}(surf.); 5 – U_{min}(surf.); 3 – (vol).

5. Analyses and discussion of the nucleation and growth kinetics

5.1. Crystal nucleation rates-homogeneous nucleation

According to the classical theory of nucleation, e.g. [17], the homogeneous nucleation rate, I_{hom}, can be written as

$$I_{hom} = 2N_l v_o \left(\frac{\sigma a^2}{kT}\right) \exp\left(-\frac{\Delta G_D + W^*}{kT}\right), \qquad (6)$$

where k is Boltzmann's constant, $N_l \cong 1/a^3$ is the number of structural (formula) units of melt with size a per unit volume, $v_o = kT/h$ is the vibration frequency of a structural unit (for typical nucleation temperatures, $v_o \cong 10^{13}$ s^{-1}), h is Planck's constant, σ is the free energy of the nucleus/melt interface per unit area, ΔG_D is the free activation energy for transport of a structural unit across the nucleus/melt interface, W^* is the work of forming a critical nucleus, i.e. the thermodynamic barrier for nucleation. For a spherical nucleus:

$$W^* = 16\pi\sigma^3/3\Delta G_v^2, \qquad (7)$$

where ΔG_v is the free energy change per unit volume of crystal.

It is often assumed that ΔG_D is close to the free activation energy of viscous flow, ΔG_η. The validity of this approximation for crystal nucleation and growth processes was demonstrated in [18,19], respectively. Hence, the kinetic term, $\exp(-\Delta G_D/kT)$, in Eq. (6) can be expressed in terms of the viscosity, η, by using of Eq. (8), derived in [20] for silicate glasses:

$$\eta = \frac{kT}{l^3} v_o^{-1} \exp\left(\frac{\Delta G_\eta}{kT}\right), \qquad (8)$$

where l has a value of the order of the Si–O bond length. The combination of Eqs. (6) and (8) results in

$$I_{hom} = 2N_l \left(\frac{\sigma a^2}{kT}\right)^{1/2} \frac{kT}{l^3\eta} \exp\left(-\frac{W^*}{kT}\right). \qquad (9)$$

Heterogeneous nucleation: In the case of heterogeneous nucleation on a melt/substrate interface, the nucleation rate expression becomes

$$I_{het} = N_{lS} \frac{kT}{l^3\eta} \exp\left(-\frac{W^*_{het}}{kT}\right), \qquad (10)$$

where $N_{lS} \cong N_l^{2/3}$ is the number of structural units adjacent to a substrate per unit area and W^*_{het} is the thermodynamic barrier for heterogeneous nucleation. When there are m substrate particles of average area s, located in a unit volume or on a unit area (in the case of surface nucleation on an active sites), Eq. (10) can written as

$$I_{het} = msN_{lS} \frac{kT}{l^3\eta} \exp\left(-\frac{W^*_{het}}{kT}\right). \qquad (10a)$$

For a nucleus of spherical cap shape the thermodynamic barrier, W^*_{het}, can be written as [21]

$$W^*_{het} = W^*\phi(\theta),$$
$$\phi(\theta) = (2 - 3\cos\theta + \cos^3\theta)/4, \qquad (11)$$

The equilibrium wetting angle θ between the nucleus and a flat substrate must satisfy the following equation resulting from the condition of mechanical equilibrium:

$$\cos(\theta) = \left(\frac{\sigma_{ms} - \sigma_{cs}}{\sigma_{cm}}\right), \qquad (12)$$

where σ_{ms}, σ_{cs} and $\sigma_{cm} \equiv \sigma$ are the interfacial free energies per unit area between melt/substrate, crystal/substrate and crystal/melt.

The combination of Eqs. (7), (10a) and (11) results in

$$I_{\text{het}} = msN_{l\text{S}}\frac{kT}{l^3\eta}\exp\left(-\frac{16\pi\sigma^3\phi(\theta)}{3\Delta G_{\text{v}}^2 kT}\right) \tag{13}$$

or

$$\ln\left(\frac{I_{\text{het}}\eta}{T}\right) = \ln A - \frac{16\pi\sigma^3\phi(\theta)}{3kT\Delta G_{\text{v}}^2},\ A = msN_{l\text{S}}\frac{k}{l^3}. \tag{13a}$$

The value of $\sigma\phi(\theta)^{1/3}$ can be obtained from the slope ($K = 16\pi\sigma^3\phi(\theta)/3k$) of a $\ln(I_{\text{het}}\eta/T)$ versus $1/T\Delta G_{\text{v}}^2$ plot by means of

$$\sigma\cdot\phi(\theta)^{1/3} = (K3k/16\pi)^{1/3}. \tag{14}$$

The interfacial free energy σ between nucleus and melt can be estimated by the following semi-empirical expression obtained by Turnbull for a number of simple liquids [22]

$$\sigma = \alpha\Delta H_{\text{m}}V_{\text{m}}^{-2/3}N_A^{-1/3},\quad \Delta H_{\text{m}} = \Delta H_{\text{v}}V_{\text{m}},$$
$$V_{\text{m}} = M/\rho_{\text{c}}, \tag{15}$$

where ΔH_{m} and ΔH_{v} are the heat of melting per mole and per unit volume of crystal, respectively, V_{m} the molar volume, N_{A} is Avogadro's number, M a molecular weight, ρ_{c} the crystal density and α is an empirical, dimensionless, coefficient. For several silicate glasses which display homogeneous nucleation, the values of α do not vary much – $0.4 < \alpha < 0.6$ [23]. The combination of Eqs. (14) and (15) results in the following equation for $\phi(\theta)$:

$$\phi(\theta) = K\frac{3kN_A\rho_{\text{c}}}{16\pi\alpha^3\Delta H_{\text{v}}^3 M}. \tag{16}$$

It is known that μ-cordierite is a metastable phase [24] and thus exact values of the heat of melting ΔH_{v} and melting point T_{m} are not available. Therefore, the following limiting values were taken from [25,26]: $T_{\text{m}} = 1423$–1590 K, $\Delta H_{\text{v}} = (7.51$–$8.39)10^8$ J/m^3, $M = 0.292$–0.585 kg/mol (depending on the building units choice) and $\rho_{\text{c}} = 2590$ kg/m^3. Thermodynamic driving force values were calculated by Eqs. (17) and (18), which normally bound the correct values for many glass systems:

$$\Delta G_{\text{v}}(T) = \Delta H_{\text{v}}(T_{\text{m}} - T)/T_{\text{m}}, \tag{17}$$

$$\Delta G_{\text{v}}(T) = \Delta H_{\text{v}}(T_{\text{m}} - T)T/T_{\text{m}}^2. \tag{18}$$

Eqs. (17) and (18) were derived under the assumption that the differences in specific heats between the crystal and liquid at constant pressure are $\Delta C_p = 0$ (Eq. (17)) or $\Delta C_p = $ constant (Eq. (18)) [27,28]. In addition, Eq. (19) was derived for the case $\Delta C_p = \Delta C_p(T_{\text{m}})$. That equation provides a good agreement with experimental values for a number of silicate glasses [29]

$$\Delta G_{\text{v}}(T) = \Delta H_{\text{v}}(T_{\text{m}} - T)/T_{\text{m}} - \Delta C_p(T_{\text{m}}) \times (T_{\text{m}} - T)^2/2T_{\text{m}}. \tag{19}$$

In the equation shown above it is assumed that the 'bulk' values of viscosity also control the molecular arrangements at the surface of the glass. Fig. 8 shows $\ln(I_{\text{v}}\eta/T)$ versus $1/T\Delta G_{\text{v}}^2$ plots calculated by Eq. (17) for different values of T_{m} and ΔH_{v}. Similar plots were calculated by Eq. (18) and Eq. (19). The corresponding values of A and K, from linear fits, are listed in Table 4 together with the values of $\sigma.\phi(\theta)^{1/3}$, $\phi(\theta)$ and σ calculated by the Turnbull Equation (Eq. (15)) with $\alpha = 0.4$. For all combinations of T_{m}, ΔH_{v} and M, which varied through a quite large range, and for different approximations for ΔG_{v}, the wetting angle function $\phi(\theta)$ is smaller than 1. It should be noted that using values of α

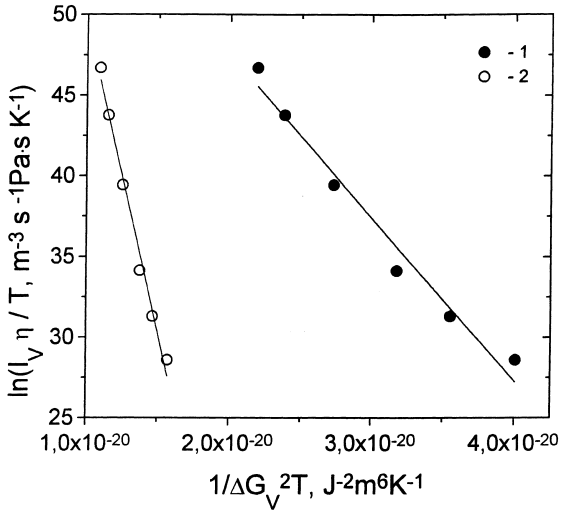

Fig. 8. $\ln(I_{\text{v}}\eta/T)$ for glass N5 as a function of $1/\Delta G_{\text{v}}^2 T$; ΔG_{v} calculated by Eq. (17): 1 – $T_{\text{m}} = 1423$ K, $\Delta H_{\text{v}} = 7.51\times10^8$ J/m^3, 2 – $T_{\text{m}} = 1590$ K, $\Delta H_{\text{v}} = 8.39\times10^8$ J/m^3.

Table 4
Thermodynamic parameters from crystal volume nucleation measurements in a cordierite glass with 8.1% TiO_2

T_m (K)	ln A, A in (J/m^6 K)	ΔH_v (J/m^3)	K (J^2 K $m)^{-6}$	$\sigma \cdot \phi^{1/3}$ (J/m^2)	σ (Eq. (15), $\alpha = 0.4$) (J/m^2)		$\phi(\theta)$		θ (grad)	
					$M = 0.292$ [a]	$M = 0.585$ [a]	$M = 0.292$ [a]	$M = 0.585$ [a]	$M = 0.292$ [a]	$M = 0.585$ [a]
$\Delta G = \Delta H_m \Delta T/T_m$										
1423	67.7	751×10^6	1.011×10^{21}	0.094	0.172	0.217	0.161	0.081	61	49
1590	87.8	839×10^6	3.827×10^{21}	0.146	0.192	0.242	0.440	0.219	85	67
$\Delta G = \Delta H_m T \Delta T/T_m^2$										
1423	84.8	751×10^6	9.293×10^{20}	0.091	0.172	0.217	0.148	0.074	59	48
1590	163.4	839×10^6	4.478×10^{21}	0.154	0.192	0.242	0.516	0.258	91	75
$\Delta G = \Delta H_m \Delta T/T - \Delta C_p(T_m)\ \Delta T^2/2T_m$										
1423	73.3	751×10^6	9.356×10^{20}	0.091	0.172	0.217	0.148	0.074	59	48
1590	104.0	839×10^6	3.591×10^{21}	0.143	0.192	0.242	0.413	0.206	83	65

[a] M is in kg/mol.

greater than 0.4 in Eq. (16) leads to even smaller values of $\phi(\theta)$. Hence, volume nucleation of μ-cordierite in TiO_2–cordierite glasses occurs by heterogeneous nucleation. This conclusion is consistent with the fact that cordierite glasses without TiO_2 or having TiO_2 contents smaller than 8 wt% only exhibit surface nucleation [30]. Moreover, it is known that liquid–liquid phase-separation is observed for TiO_2 contents higher than 8 wt% and the primary crystal phase at 800°C is Al_2TiO_5 [26]. Hence, one can assume that volume nucleation in the glass having 8.1 wt% TiO_2 (N5) is probably catalyzed by Al_2TiO_5.

It is obvious that the total number of structural units, adjacent to the substrate particles, m.s.$N_{l\mathrm{S}}$, is always smaller than $N_l \approx 1/a^3 = \rho_c N_A/M$. Replacing the term m.s.$N_{l\mathrm{S}}$ in Eq. (13a) by N_l, one can write the following inequality $\ln A < \ln N_1 + \ln(k/l^3)$. For $\rho_c = 2590$ kg/m^3, $l = 2 \times 10^{-10}$m and $M = 0.292$–0.585 kg/m^3, $\ln(A,\ \mathrm{J/m^6\ K}) < 77$–$78$. However, according to Table 4, this inequality holds only with $T_m = 1423$ K. Therefore, in the following analysis, we use $T_m = 1423$ K as more probable equilibrium temperature.

Surface nucleation rates, I_S, are given per unit area while volume nucleation rates, I_v, are given per unit volume. Thus, to compare the values of surface and volume quantities, it is necessary to solve the problem of dimensions. In fact, surface nucleation can be assumed to occur in a narrow layer, immediately adjacent to the glass surface. In the case of nucleation on some active surface sites, an effective volume involved in the surface nucleation process can be estimated as $V = \mathrm{ms}L$, where L is an effective layer thickness. It should be noted that V is the volume per unit area of surface layer. Hence, by dividing Eq. (13) for the surface nucleation rate by V, we obtain a surface nucleation rate i_S having the same dimension of the volume nucleation rate.

$$i_S = I_{het}/V = \frac{N_l S}{L}\frac{kT}{l^3\eta}\ \exp\left(-\frac{16\pi\sigma^3\phi(\theta)}{3\Delta G_v^2 kT}\right), \quad (20)$$

or

$$\ln\left(\frac{i_S\eta}{T}\right) = \ln\ \tilde{A} - \frac{16\pi\sigma^3\phi(\theta)}{3k}\frac{1}{\Delta G_v^2 T},\ \tilde{A} \equiv \frac{N_{l\mathrm{S}}k}{Ll^3}. \quad (20a)$$

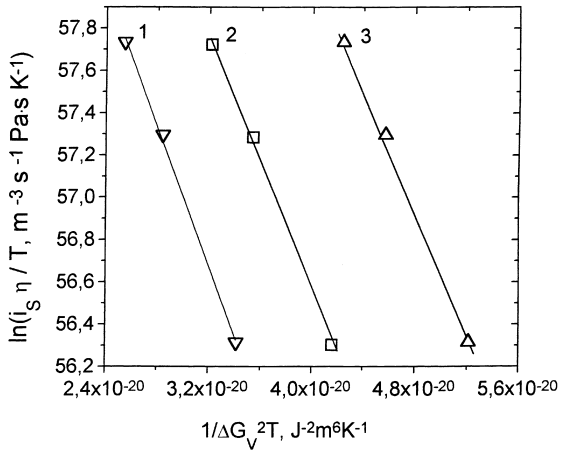

Fig. 9. $\ln(i_S\eta/T)$ for glass N5 as a function of $1/\Delta G_v^2 T$; $T_m = 1423$ K, $\Delta H_v = 8.39 \times 10^8$ J/m^3; ΔG_v calculated by: 1 – Eq. (17), 2 – Eq. (19), 3 – Eq. (18).

It is reasonable to assume that L has the order of a molecular jump distance $\sim 2 \times 10^8$ cm. For a rough estimate of V, the following values were used: $m = 10^8$ cm^{-2} (10 times more than the observed values) and $s = 3.14 \times 10^{-10}$ cm^2 (the average particle radius is $\sim 10^{-5}$cm). It should be emphasized that the choice of V affects only the value of $\tilde{A}$ in Eq. (20a) but not the slope K of the $\ln(i_S\eta/T)$ versus $1/\Delta G_v^2 T$ plots of Fig. 9, which is determined by $\sigma^3 \cdot \phi(\theta)$. The surface nucleation parameters calculated from the data of Fig. 9 are listed in Table 5. As would be expected for heterogeneous nucleation, the values of $\phi(\theta)$ are much smaller than 1.0.

In the case of nucleation on a clean glass/atmosphere interface, the term $(\sigma_{ms} - \sigma_{cs})$ in Eq. (12) should be replaced by $(\sigma_m - \sigma_c)$, where σ_m and σ_c are the surface energies of the melt/atmosphere and crystal/atmosphere interfaces, respectively. It should be expected that the following inequality holds $\sigma_c/\sigma_m \geqslant 1$ [1] [4]. Then the equilibrium wetting angle between the nucleus and a pristine glass surface should be $\theta \geqslant 90°$. Thus, the inequality $\theta < 90°$ obtained for surface nucleation in cordierite glass (see Table 5) supports the hypotheses of nucleation on some active substrates on the glass surface but not on virgin glass surfaces.

[1] For a number of metals and alloys $\sigma_c/\sigma_m = 1.33$ [31], 1.15 [32], 1.18 [33].

5.2. Crystal growth velocity

Three standard models [34], resulting from different views of the nature of the crystal/melt interface, are usually employed to describe the crystal growth kinetics in glasses: the screw dislocation model, the continuous growth model and the bidimensional surface nucleation growth model.

5.3. The screw dislocation model

The screw dislocation growth model views the crystal/melt interface as imperfect on an atomic scale, with growth taking place at steps sites provided by screw dislocations intersecting the interface. The crystal growth rate U is given by

$$U = \frac{fakT}{l^3\eta}\left[1 - \exp\left(-\frac{V\Delta G_v}{kT}\right)\right], \tag{21}$$

where $f \sim \Delta G_v$ is the fraction of atomic sites on the crystal surface where atoms or molecules can be attached, $V = V_m/N_A$ is the molecular volume.

The reduced crystal growth velocity, U_R, is commonly used at the analysis of the mechanism growth

$$U_R \equiv U\eta \Big/ \left[1 - \exp\left(-\frac{V\Delta G_v}{kT}\right)\right], \quad U_R \sim T\Delta G_v. \tag{22}$$

5.4. The continuous growth model

In the framework of this model, the interface is imaged as rough on atomic scale and all sites on the interface are equivalent growth sites. The growth rate is expressed by Eq. (21) with $f \sim 1$.

5.5. The bidimensional (secondary) surface nucleation growth model

The surface nucleation growth model was elaborated for crystal/liquid interfaces that are

Table 5
Thermodynamic parameters from surface nucleation measurements in a cordierite glass with 8.1 wt% TiO_2

$\ln \tilde{A}, A$ (J/m^6 K)	K (J^2 K m^{-6})	$\sigma \cdot \phi^{1/3}$ (J/m^2)	σ (Eq. (15), $\alpha = 0.4$) (J/m^2)		$\phi(\theta)$		θ (grad)	
			$M = 0.292$ [a]	$M = 0.585$ [a]	$M = 0.292$ [a]	$M = 0.585$ [a]	$M = 0.292$ [a]	$M = 0.585$ [a]
$\Delta G = \Delta H_m \Delta T / T_m$								
64.2	1.308×10^{20}	0.047	0.172	0.217	0.020	0.010	34	28
$\Delta G = \Delta H_m T \Delta T / T_m^2$								
66.3	1.175×10^{20}	0.046	0.172	0.217	0.019	0.009	34	28
$\Delta G = \Delta H_m \Delta T / T - \Delta C_p(T_m)\ \Delta T^2 / 2T_m$								
64.9	1.212×10^{20}	0.046	0.172	0.217	0.019	0.009	34	28

$T_m = 1423$ K, $\Delta H_v = 751 \times 10^6$ J/m^3.
[a] M is in kg/mol.

smooth on an atomic scale and free of intersecting screw dislocations. Crystal growth occurs by surface nucleation and lateral spread of bidimensional nuclei on the interface. The growth rate is expressed by the following equation [34]

$$U = C\frac{T}{\eta}\exp\left(-\frac{B}{T\Delta G_v}\right), \tag{23}$$

which can be written as

$$\ln(U\eta/T) = \ln C - B/T \cdot \Delta G_v, \tag{23a}$$

where C depends weakly on the temperature as compared with $\exp(-B/kT)$ and η. When the secondary nuclei grow across the interface in times that are short compared with the time period between nucleation events, one has a 'small' crystal case. In that case B takes the following form:

$$B = \pi a \sigma^2 / k. \tag{24}$$

In the opposite situation, one has a 'large crystal' case, for which

$$B = \pi a \sigma^2 / 3k \tag{24a}$$

Fig. 10 present the results of the crystal growth analysis in the framework of the theory briefly described above. The values of T_m, ΔH_m, M and ρ_c used in the calculations are indicated in the figure captions.

According to (Eqs. (17), (18) and (22)), in the case of screw dislocation growth, a plot U_R versus $T \cdot \Delta T$ or $T^2 \cdot \Delta T$ would be a straight line of positive slope passing through the origin. It can be seen that the data of Fig. 10(a) and (b) cannot be described by Eq. (22). Hence, the growth kinetics of μ-cordierite in the 8.1 wt% TiO_2 cordierite glass cannot be described by the screw dislocation model. On the other hand, according to the secondary 2D nucleation growth model (Eq. (23a)), a $\ln(U\eta/T)$ versus $1/T\Delta G_v$ plot would be a straight line of negative slope. Indeed, the data presented

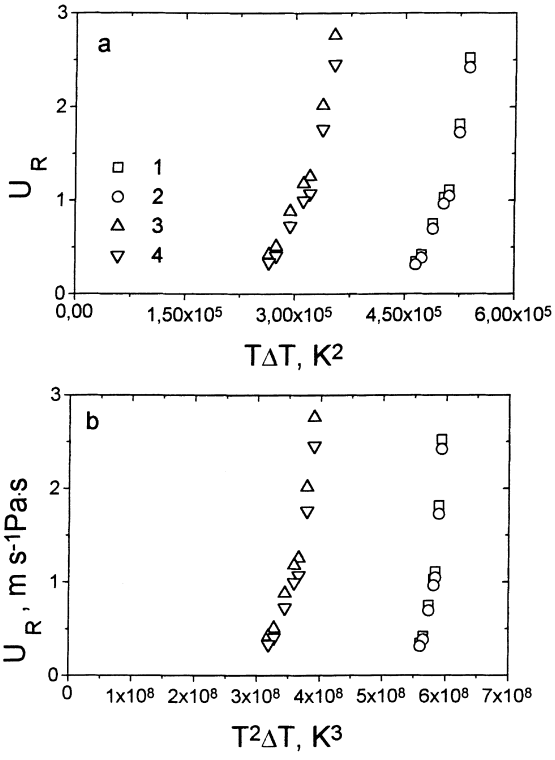

Fig. 10. Reduced crystal growth velocity U_R in glass N5 (a) versus $T\Delta T$ and (b) versus $T^2\Delta T$: 1, 2 – $T_m = 1590$ K, $\Delta H_v = 8.39 \times 10^8$ J/m^3; 3, 4 – $T_m = 1423$ K, $\Delta H_v = 7.51 \times 10^8$ J/m^3. 1, 3 – $M = 0.292$ kg/mol; 2, 4 – $M = 0.585$ kg/mol.

in Fig. 11 are well fitted by a line with negative slope. Thus we conclude that the *secondary 2D nucleation growth mechanism* is the most probable mechanism governing crystal growth in our glass.

The secondary surface nucleation growth model allows one to calculate the surface energy σ of the crystal/glass interface, from the slope of $\ln(U\eta/T)$ on $1/T\Delta G_v$ plots (see Eqs. (23a), (24) and (24a)). Table 6 lists the surface free energy values for the cases of 'small' and 'large' crystal, calculated from the plots of Fig. 11, together with the calculated values of σ obtained from the Turnbull Equation (15) with $\alpha = 0.4$. In general, the surface energy values independently obtained from crystal growth data are smaller than the calculated values by Eq. (15), which are based on volume nucleation data for several silicates. According to Table 6, the use of $M = 0.292$ kg/mol (large crystal case) provides the best agreement between the calculated and experimental values of σ.

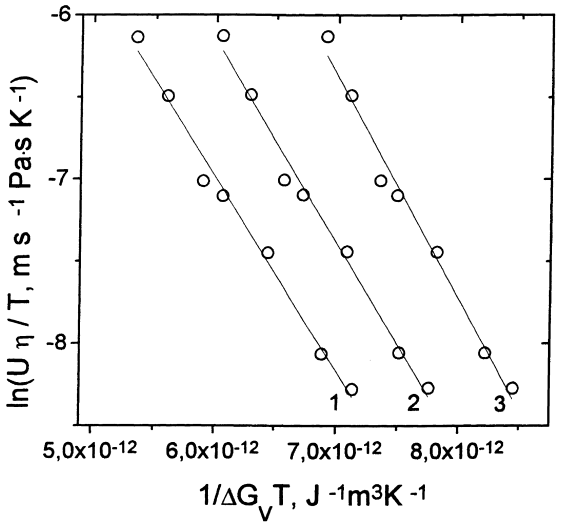

Fig. 11. ln $(U\eta/T)$ for glass N5 versus $1/\Delta G_v T$; ΔG_v calculated by: 1 – Eq. (17), 2 – Eq. (19), 3 – Eq. (18), with $T_m = 1423$ K and $\Delta H_v = 7.51 \times 10^8$ J/m^3.

Fig. 12 illustrates the main results of the analysis of nucleation and growth data in the 8.1 wt% TiO_2 glass. Using $T_m = 1423$ K (see 5.1), $M = 0.292$ kg/mol, $\Delta H_v = 7.51 \times 10^8$ J/m^3, viscosity data and the experimental (fitted) values of the pre-exponential factors A, $\tilde{A}$ and C, it is possible to plot fitted curves of the heterogeneous volume nucleation rate, $I_v \equiv I_{het}$ (Eq. (13), heterogeneous surface nucleation rate, i_S (Eq. (20) and crystal growth rate, U (Eq. (23). Such fitted curves are shown in Fig. 12 together with the experimental data. For comparison we also plot what would be the homogeneous nucleation rate I_{hom} (Eq. (9)) using $\alpha = 0.4$ and the theoretical value of the pre-exponential constant.

In passing from homogeneous to heterogeneous nucleation, and thus decreasing ϕ, leads to larger values of nucleation rate and shifts its maximum to higher temperatures. As this takes place, the maximum temperature is flattened and approaches that of the crystal growth rate. The last points were also noted in Ref. [25].

Table 6
Thermodynamic parameters from crystal growth measurements in a cordierite glass with 8.1 wt% TiO_2

M (kg/mol)	B (Jm^{-3}K)	σ (J/m^2)		
		Small crystal	Large crystal	Eq. (16), $\alpha = 0.4$
$\Delta G = \Delta H_m \Delta T/T_m$				
0.292	1.176×10^{12}	0.095	0.165	0.172
0.585	1.176×10^{12}	0.085	0.147	0.217
$\Delta G = \Delta H_m T\Delta T/T_m^2$				
0.292	1.358×10^{12}	0.102	0.177	0.172
0.585	1.358×10^{12}	0.091	0.157	0.217
$\Delta G = \Delta H_m\ \Delta T/T_m - \Delta C_p \Delta T^2/2T_m$				
0.292	1.230×10^{12}	0.097	0.168	0.172
0.585	1.230×10^{12}	0.087	0.151	0.217

$T_m = 1423$ K, $\Delta H_v = 751 \times 10^6$ J/m^3.

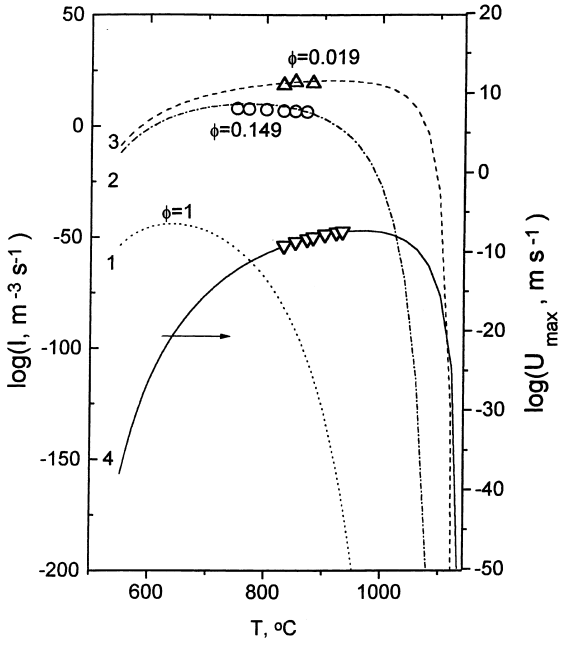

Fig. 12. I_{hom} (1), I_v (2), i_S (3), and U (4) for glass N5 as a function of temperature: lines = fitted curves, points = experimental data.

The analysis performed does not take into account the nature of the catalysing substrates. When the catalyzing particles are equal in the volume and on the surface, it is expected that the values of ϕ are also equal. However, the values of ϕ obtained here for surface and volume nucleation (see Tables 4 and 5) differ approximately 8 times. Hence, it is natural to assume that the active surface sites are not equal to those in the interior of the glass. The nucleation process on the polished surfaces is much more complex than that in the glass bulk. The effect of TiO_2 on the surface nucleation rates should be closely coupled to the peculiarities of the polished surface and to the polishing process. Here, it is worth reminding that this effect was not observed in the case of nucleation on fractured surfaces (Section 3.1.2). In this connection we first believed that TiO_2 could affect the microhardness of the glass and correspondingly the polishing of glass. However, according to Table 3, the microhardness does not change appreciably with TiO_2 content.

One could also speculate that a decreased thermodynamic driving force, ΔG_v, in Eq. (13) due to the elastic strain energy, ΔG_e, could arise from the difference between the molar volumes of glass and crystal [21]. The value of ΔG_e in the immediate vicinity of the external glass surface is less than that in the glass bulk. Hence, the thermodynamic driving force for the volume nucleation could be less than that for the surface nucleation. It can be shown that if this effect is accounted for, the calculated values of ϕ for volume and for surface nucleation will approach each other. It should be emphasised, however, that the problem of elastic strain is directly related with the relation between the time of formation of a critical nucleus, τ_n, and the time for stress relaxation ($\tau_s = \eta/G$, where G is the shear modulus). In general, however, $\tau_s \ll \tau_n$. Hence, the effect of stresses can be neglected.

At constant values of the kinetic barrier (or η), number and average size of catalyzing particles, the heterogeneous nucleation rate is controlled mainly by the thermodynamic barrier W^*_{het}. If the number of catalyzing particles increases with the TiO_2 content the nucleation rate also increases. Since, according to the nucleation rates analysis, W^*_{het}(volume) > W^*_{het}(surface), one can assume a situation where the volume nucleation rate is too small to be observed experimentally while the surface nucleation can be measured. It is possible that this situation applies for glasses having less than 8wt% TiO_2.

6. Conclusions

Surface nucleation and volume nucleation rates of μ-cordierite crystals were measured in the same temperature range for a TiO_2–cordierite glass. Crystal growth velocity of μ-cordierite crystals is well fitted by the bidimensional surface nucleation growth model. The maximum of surface nucleation rate takes place at a temperature considerably higher that of volume nucleation rate maximum. Both occur by heterogeneous nucleation. Nucleation on polished surfaces and in the glass volume is strongly affected by TiO_2 content. The significant difference in the average crystal/substrate wetting angles for surface and volume

nucleation results from the different nature of active catalyzing sites for the two processes. It is likely that Al_2TiO_5 crystals induce volume crystallization of μ-cordierite, while surface crystallization is affected by TiO_2, defects and remnants of polishing power.

Acknowledgements

The authors acknowledge the financial assistance provided by CNPq/RHAE (Grant No.360246/96-6). We are also grateful to Dr V. Klyev for viscosity data, and for the critical comments of Drs V. Filipovich and N. Yuritsin. Funding by PRONEX and FAPESP were fully appreciated.

References

[1] E.D. Zanotto, J. Non-Cryst. Solids 129 (1991) 183; E.D. Zanotto, Ceram. Trans. 30 (1993) 65.
[2] R. Müller, S. Reinsch, W. Pannhorst, Glastech. Ber. 69 (1996) 12.
[3] J. Deubener, R. Brückner, H. Hessenkemper, Glastech. Ber. 65 (1992) 256.
[4] V. Filipovich, V. Fokin, N. Yuritsin, A. Kalinina, Thermochem. Acta 280&281 (1996) 205.
[5] G. Völksch, K. Heide, J. Non-Cryst. Solids 218 (1997) 119.
[6] N.D. Mora, E.D. Zanotto, E.C. Ziemath, Phys. Chem. Glasses 37 (1996) 258.
[7] J. Schmelzer, J. Möller, I. Gutzow, R. Pascova, R. Müller, W. Pannhorst, J. Non-Cryst. Solids 183 (1995) 215.
[8] I. Szabo, W. Pannhorst, M. Rappensberger, Investigation on the effect of surface treatment and annealing on the surface crystallization of the $MgO–Al_2O_3–SiO_2$ glass, in: Proceedings of the XVI International Congress on Glass, Madrid, 1992, vol.5, pp. 119.
[9] N.S. Yuritsin, V.M. Fokin, A.M. Kalinina, V.N. Filipovich, Ceram. Trans. 30 (1993) 379.
[10] Z. Strnad, R.W. Douglas, Phys. Chem. Glasses 14 (1973) 33.
[11] U. Köster, Mater. Sci. Eng. 97 (1988) 233.
[12] S. Toshew, I. Gutzow, Krist. Tech. 7 (1972) 43.
[13] G. Steinbrink, PhD thesis, Dortmund, 1992.
[14] K. Lakshmi Narayan, K.F. Kelton, C.S. Ray, J. Non-Cryst. Solids 195 (1996) 148.
[15] V.M. Fokin, N.S. Yuritsin, V.N. Filipovich, A.M. Kalinina, J. Non-Cryst. Solids 219 (1997) 37.
[16] V.M. Fokin, A.M. Kalinina, V.N. Filipovich, I.G. Polyakova, Glass Phys. Chem. 12 (1986) 480.
[17] J.W. Christian, The Theory of Transformation in Metals and Alloys, Part 1, Pergamon Press, Oxford, 1981; P.F. James, in: J.H. Simmons, D.R. Uhlmann, G.H. Beall (Eds.), Advances in Ceramics, vol. 4, Nucleation and Crystallization in Glasses, Am. Ceram. Soc., Columbus, OH, 1982, p. 1.
[18] N. Diaz-Mora, E.D. Zanotto, V.M. Fokin, Phys. Chem. Glasses 39 (2) (1998) 91.
[19] V.M. Fokin, A.M. Kalinina, V.N. Filipovich, J. Cryst. Growth 52 (1981) 115.
[20] V.N. Filipovich, Glass Phys. Chem. 1 (1975) 426.
[21] I. Gutzow, J. Schmelzer, The Vitreous State, Springer, Berlin, 1995.
[22] D. Turnbull, J. Appl. Phys. 21 (1950) 1022.
[23] S. Manrich, E.D. Zanotto, Cerâmica 41 (1995) 105.
[24] W. Schreyer, J.F. Schairer, Z. Kristallogr. 116 (1961) 60.
[25] R. Müller, R. Naumann, S. Reinsch, Thermochim. Acta 280–281 (1996) 191.
[26] T. Hübert, R. Müller, M. Kirsch, Silicattechnik 40 (1989) 205.
[27] K.F. Kelton, Sol. Stat. Phys. 45 (1991) 75.
[28] J.D. Hoffman, J. Chem. Phys. 29 (1958) 1192.
[29] V.N. Filipovich, A.M. Kalinina, V.M. Fokin, Problem of relation between structure of glass and its abillity to volume crystallization, in: E.A. Porai-Koshits (Ed.), Stekloobraznoe Sostoyanie, Leningrad, 1983, p. 124 (in Russian).
[30] R.Ja. Khodakovskaya, Chemistry of Ti-doped Glasses and Glass Ceramic, Moscow, 1978 (in Russian).
[31] J.W. Taylor, J. Inst. Met. 86 (1958) 456.
[32] S.N. Zadumkin, A.A. Karashaev, Nalchik 85 (1965) (in Russian).
[33] W.K. Tayson, W.A. Miller, Surf. Sci. 62 (1977) 267.
[34] D.R. Uhlmann, in: J.H. Simmons, D.R. Uhlmann, G.H. Beall, (Eds.), Advances in Ceramics, vol. 4, Nucleation and Crystallization in Glasses, Am. Ceram. Soc., Columbus, OH, 1982, p. 80.